

## Deoxyglucose Analysis of Retinotopic Organization in Primate Striate Cortex

**Abstract.** We have anatomically analyzed retinotopic organization using the  $^{14}\text{C}$ -labeled 2-deoxy-D-glucose method. The method has several advantages over conventional electrophysiological mapping techniques. In the striate cortex, the anatomical substrate for retinotopic organization is surprisingly well ordered, and there seems to be a systematic relationship between ocular dominance strips and cortical magnification. The 2-deoxyglucose maps in this area appear to be largely uninfluenced by known differences in long-term metabolic activity. This method should prove useful in analyzing retinotopic organization in various visual areas of the brain and in different species.

In the primary visual areas of the brain, cells are anatomically arranged so that stimuli in adjacent positions in the visual field activate nearby neurons. Since this orderly arrangement of neurons in the brain reflects the arrangement of the visual image on the photoreceptor grid of the retina, it has been called a "retinotopic" organization.

The retinotopic organization has traditionally been studied physiologically: information about receptive field location is collected from many different recording sites, and an idealized map is interpolated between sampled sites. Though this approach has been of great value, it is time-consuming, subject to various interpolation and resolution inaccuracies, and able to yield relatively little of the potential information from each animal.

We have examined the retinotopic organization anatomically, in a novel application of the 2- $^{14}\text{C}$ deoxy-D-glucose (2DG) method developed by Sokoloff *et al.* (1). This method is in many ways superior to conventional mapping methods, since the 2DG map gives a sharply detailed view of the complete retinotopic organization in many visual areas in each animal. The scope and clarity of our results have allowed us to address many unresolved questions about the retinotopic organization in the primate striate cortex. The 2DG method is especially useful here, because it allows a clear and immediate view of the anatomical relation between the overall retinotopic organization and the local columnar functional organization of this cortical area. Although we report here only on the primate striate cortex, we have also seen good 2DG maps in subcortical and extrastriate cortical areas and in other mammalian species. It is therefore likely that the present approach will find a broad usefulness.

The visual patterns used were produced using an image processing system (Lexidata) driven by a computer (NOVA 4) and presented on a display monitor (Tektronix 654). The patterns consisted of eight rays and three to five concentric

rings equally spaced on a logarithmic scale (Fig. 1A). The rings and rays were composed of small checks that were flickered between black and white at 3 Hz. All patterns were presented monocularly. The basic experimental procedures have been described elsewhere (2, 3). Macaque monkeys were anesthetized, intubated, pharmacologically paralyzed, and connected to a respirator. The animal's head was held rigidly but painlessly with a plastic headset implanted a week earlier. Standard optical procedures were used to bring the stimulus screen to a focus on the animal's retina. At the onset of the experiment, the animal was injected with 25  $\mu\text{Ci}$  of  $^{14}\text{C}$ -labeled 2DG per kilogram of body

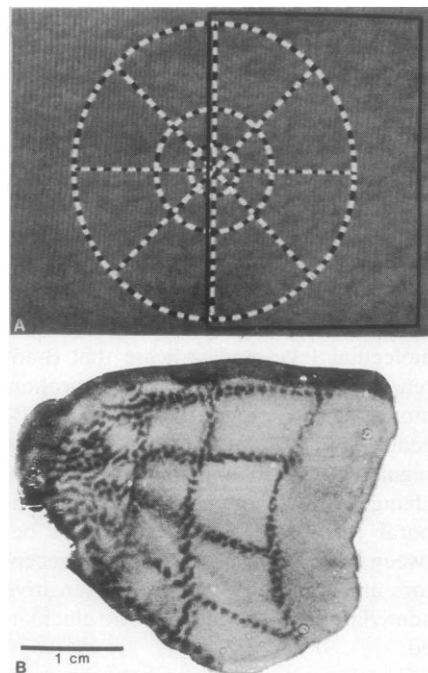


Fig. 1. (A) One of the visual stimuli used. The solid black rectangle encloses that portion of the visual stimulus that stimulated the region of striate cortex shown in (B). (B) Pattern of brain activation produced by the visual stimulus shown in (A), as revealed by 2DG. This is an autoradiograph from a single flat-mounted tissue section (mostly from layers 4B and 4C). About half of the total surface area of the macaque striate cortex can be seen.

weight, and the visual pattern was continuously presented for the next 25 to 30 minutes. The animal was then given an overdose of barbiturate and lightly perfused. In order to see the maps in a single histological section, we have developed a flat-mount procedure for smoothing out the convoluted surface of the cortex. Sections were then cut parallel to the plane of the flat-mounted cortical surface. To monitor possible distortion during flat-mounting and sectioning, four holes were made through the cortex in a measured grid *in vivo*. Measurements in the final sections showed distortion to be less than 3 percent. Subsequent autoradiographic processing was standard, with modifications to permit cytochrome oxidase reaction of the autoradiographed sections.

A typical 2DG map of the striate cortex is shown in Fig. 1B. The overall ring-and-ray structure of the half of the visual stimulus projecting to that cortex (Fig. 1A) is evident in the resultant 2DG pattern. The blackened segments in the 2DG map correspond to portions of ocular dominance strips, since only one eye was stimulated. The counterphase-flickered check pattern within the rings and rays was spatially complex, and thus appears to have produced 2DG uptake within most or all of the ocular dominance strip representing that portion of the visual field. In one animal, the stimulus was composed of solid rings and rays, which were therefore distinctly oriented in a local region. In this case the 2DG map was dotlike in all layers except layer 4C, presumably reflecting an intersection of ocular dominance and orientation columns (4).

Recently, spotlike differences in long-term endogenous metabolic capacity (as reflected by levels of cytochrome oxidase) have been discovered in the primate striate cortex (5) (Fig. 2A), and it was originally thought that visually stimulated uptake of 2DG might be confounded with these long-term differences. To the extent that this is true, the visually stimulated 2DG maps will be obscured by visually nonspecific 2DG uptake in these regions of high cytochrome oxidase activity. However, this seems to be a quantitatively minor effect in the macaque. Densitometric comparisons were made of 2DG uptake in visually stimulated and unstimulated portions of single large sections through lower layer 3 (the layer of maximum cytochrome oxidase inhomogeneity). Differential 2DG uptake due to endogenous differences in metabolic capacity was found to be only 2 percent of that due to visual stimulation (Fig. 2B).

One of the most striking aspects of the 2DG maps is the unexpected sharpness of the borders between visually stimulated and nonstimulated regions. By measuring the fall-off in autoradiographic density along the long axis of the ocular dominance strips with a microdensitometer, it was possible to quantify the sharpness of the retinotopic borders (6). Figure 2C shows a section taken from layer 4c in which the average half-amplitude of the fall-off in density is about 100  $\mu\text{m}$ . (For comparison, our best estimate of the visual resolution limit of a monkey at this eccentricity is about 1.5 minutes of arc, a value that would also correspond to about 100  $\mu\text{m}$  of cortex in this animal at the same eccentricity.) The sharpness of the pattern in other cortical layers was not greatly different (Fig. 2B). The degree of retinotopic order in the 2DG maps seems greater than one would have predicted from reports of wide scatter of single-unit receptive field loci within a given striate area (7, 8). This discrepancy may arise from differences in the cellular locus of 2DG and single-unit signals (9), possible nonlinearities in 2DG uptake, or both. At any rate, the discrete nature of the 2DG map makes feasible a more detailed analysis of retinotopic organization than has previously been possible.

The spatial transformation of the visual field onto the striate cortex has been represented analytically as a complex logarithmic conformal mapping (10). In this model, equal distances in the visual field are expanded logarithmically in the striate cortex as the foveal representation is approached. To a first approximation, our results confirm this: concentric rings spaced in logarithmically equal steps in the visual field (Fig. 1A) produce more equally spaced bands in the striate cortex (Fig. 1B). Similarly, the widths of the rays (which are equal across the extent of the stimulus) are expanded in the cortex toward the foveal projection (Fig. 1B). From 2DG autoradiographs, we calculated the reciprocal of the cortical magnification factor (CMF) as a linear function of eccentricity (11). In two monkeys, we averaged over all ring and ray segments ( $N = 47$ ) from 0 to 10 degrees and found the  $\text{CMF}^{-1}$  to be  $0.077 \text{ deg/mm} + .082 E/\text{mm}$ , where  $E$  is the eccentricity in degrees. These figures agree with previous electrophysiological results (7, 12, 13). Closer inspection of our data, however, reveals certain local variations in the CMF, which seem to be related to the direction ocular dominance strips run through the striate cortex.

Ocular dominance and orientation columns have been demonstrated both

physiologically and anatomically (4, 14). Similar evidence has been presented for spatial frequency columns as well (3, 15). These columnar organizations seem to be arranged so that a small region of the cortex (corresponding to a local region of the visual field) contains cells tuned to all orientations and spatial frequencies for each eye. Such a collection of cells can be termed a cortical module. If (for example) a square patch of visual space projected isotropically onto a cortical module, a square cortical region would be activated by input from the corresponding retinal region (16). However, the space required to completely map out each of the orientation, ocular dominance, and spatial frequency dimensions may not be equal. This could result in a square patch of visual space mapping onto, say, a rectangular region of the cortex; in this case the CMF would differ in different directions across cortex; it would be anisotropic.

We did find the CMF to be anisotropic

[a feature not described by a complex logarithmic map (10)]. When we compared the length of different map segments subtending the same eccentricities, we found that the overall CMF along a direction perpendicular to the ocular dominance strips was greater than that parallel to the ocular dominance strips (compare Fig. 2C with Fig. 2D). The increase in the overall CMF appears to be due to a duplication of input maps (one for each eye) in the direction perpendicular to ocular dominance strips. If each eye were mapped isotropically and separately in the two ocular dominance sections of a module, a square in visual space would be mapped into a 2:1 rectangle on the cortex. However, the overall distortion was less than 2:1, so the local CMF (within the ocular dominance strip from one eye) must be decreased perpendicular to the strips (17, 18).

The ocular dominance strips intersect the vertical meridian perpendicularly, but run much more parallel to the hori-

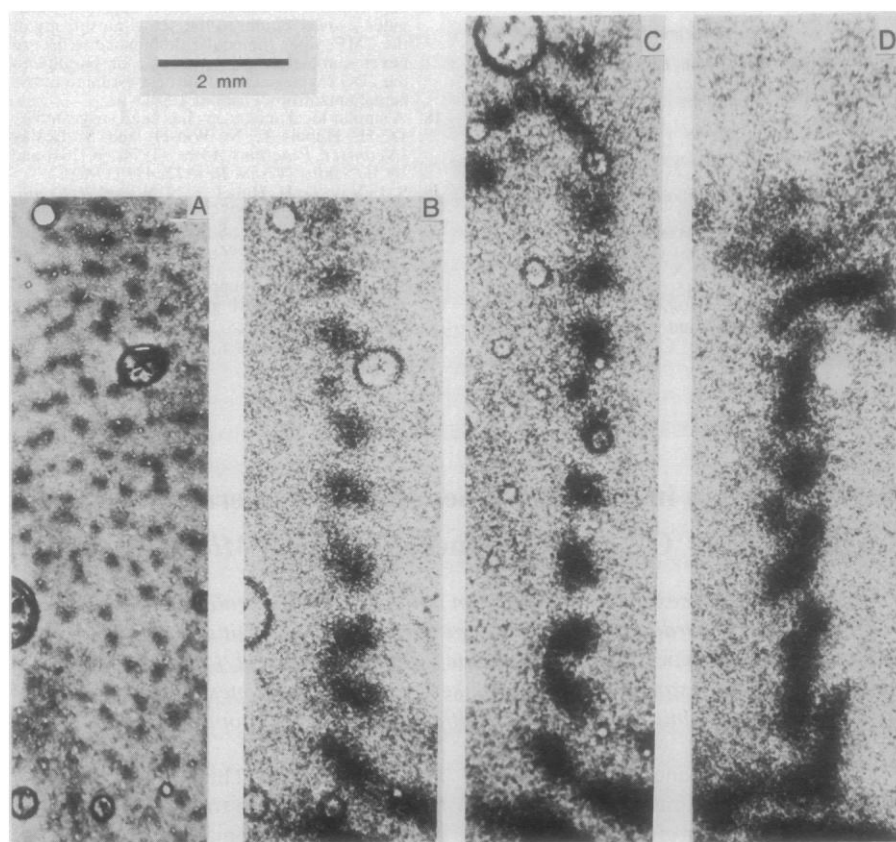


Fig. 2. (A) Close-up of the cytochrome oxidase pattern from lower layer 3 in the striate cortex of the animal shown in Fig. 1B. (B) A 2DG map from the same portion of the same tissue section as shown in Fig. 2A (note that the circular bubble artifacts are identical). The pattern of metabolic activity as shown by the 2DG in this figure differs from that shown by cytochrome oxidase in (A). (C) A 2DG map of the same ray segment as in (B), but from a different cortical layer (layer 4C). (D) A 2DG map of a ray segment that is symmetrical in the visual field to that shown in (C). Both are oblique ray segments mapped across the same eccentricities in the visual field, they are taken from the same section of the same hemisphere, and they are shown at the same scale. The segment shown in (D) happened to cross ocular dominance strips running roughly parallel to the 2DG map segment, and the segment shown in (C) happened to fall on ocular dominance strips running perpendicular to the 2DG segment. Since the cortical map is expanded perpendicular to the ocular dominance strips, the segment shown in 2C is longer.

zontal meridian (19). Therefore, the differential expansion seen along the vertical meridian in all the 2DG maps (for example, Fig. 1B) (20) is only a special case of an expansion of the cortical map perpendicular to the ocular dominance strips. This relationship resolves what would otherwise be a problem, namely that the vertical meridian is mapped over a longer distance around almost all of the elliptical circumference of the striate cortex, whereas the horizontal meridian lies along a shorter straight line connecting the ends of that ellipse (13).

ROGER B. H. TOOTELL

Department of Psychology, University of California, Berkeley 94720

MARTIN S. SILVERMAN

Department of Physiology, University of California, San Francisco 94143

EUGENE SWITKES

Committee on Psychobiology, Division of Natural Sciences, University of California, Santa Cruz 95064

RUSSELL L. DE VALOIS

Department of Psychology, University of California, Berkeley

#### References and Notes

1. L. Sokoloff, C. Reivich, C. Kennedy, M. H. Des Rosiers, C. S. Patlack, K. D. Pettigrew, O. Sakurada, M. Shinohara, *J. Neurochem.* **28**, 897 (1977).
2. R. L. De Valois and P. L. Pease, in *Methods in Physiological Psychology*, R. F. Thompson, Ed. (Academic Press, New York, 1973), p. 95.
3. R. B. Tootell, M. S. Silverman, R. L. De Valois, *Science* **214**, 813 (1981).
4. D. H. Hubel, T. N. Wiesel, M. P. Stryker, *J. Comp. Neurol.* **177**, 361 (1978).
5. A. L. Humphrey and A. E. Hendrickson, *Soc. Neurosci. Abstr.* **6**, 315, 1980; A. E. Hendrickson, in *Cytochemical Methods in Neuroanatomy*, V. Chan-Palay and S. Palay, Eds. (Liss, New York, 1982); J. C. Horton and D. H. Hubel, *Soc. Neurosci. Abstr.* **6**, 315 (1980); *Nature (London)* **292**, 762 (1981).
6. Since there is no evidence for orientation or spatial frequency columns in layer 4C, autoradiographic measurements made within an ocular dominance strip in this layer should be a true measure of retinotopic scatter.
7. D. H. Hubel and T. N. Wiesel, *J. Comp. Neurol.* **158**, 295 (1974).
8. K. Albus, *Exp. Brain Res.* **24**, 159 (1975). Somewhat less scatter is reported by B. M. Dow, A. Z. Snyder, R. G. Vautin, and R. Bauer [*ibid.* **44**, 213 (1981)].
9. F. R. Sharp, *Brain Res.* **110**, 127 (1976); W. J. Schwartz, C. B. Smith, L. Davidsen, H. Savaki, L. Sokoloff, M. Mata, D. J. Fink, H. Gainer, *Science* **205**, 723 (1979).
10. E. L. Schwartz, *Vision Res.* **20**, 645 (1980).
11. The cortical magnification factor is the amount of cortex devoted to a given region of visual space. Since the cortex is relatively uniform in thickness, and has been assumed isotropic, the CMF has been described in millimeters along the surface of cortex per degrees of eccentricity in the visual field. It is often more convenient to plot the reciprocal of the CMF, since  $CMF^{-1}$  is approximately linear with eccentricity.
12. S. A. Talbot and W. H. Marshall, *Am. J. Ophthalmol.* **24**, 1255 (1941).
13. P. M. Daniel and D. Whitteridge, *J. Physiol. (London)* **159**, 203 (1961).
14. For review see D. H. Hubel and T. N. Wiesel, *Proc. R. Soc. London Ser. B* **198**, 1 (1977).
15. R. B. Tootell, M. S. Silverman, E. Switkes, R. L. De Valois, *Soc. Neurosci. Abstr.*, in press; M. S. Silverman, R. B. H. Tootell, R. L. De Valois, *ibid.* **7**, 356, 1981.
16. For simplicity, we ignore the distortion of a square in the cortex as a result of the quasi-logarithmic expansion.
17. The ratio of the lengths shown in Fig. 2, C and D, is about 1.25:1. This measure (and similar data from comparison of other segments) provides a lower bound to the actual anisotropy of the CMF, since the ocular dominance strips are never completely perpendicular or parallel to the 2DG ray segments. Our best estimate of the actual anisotropy is about 1.5:1.
18. A similar local anisotropy has been suggested by D. H. Hubel, T. N. Wiesel, and S. LeVay [*Neurosci. Programs Abstr.* (1974), p. 264] and by B. Sakitt, [*Vision Res.* **22**, 417 (1982)].
19. S. LeVay, D. H. Hubel, T. N. Wiesel, *J. Comp. Neurol.* **159**, 559 (1975).
20. R. B. H. Tootell, M. S. Silverman, E. Switkes, R. L. De Valois, *Invest. Ophthalmol. (Suppl.)* **12**, 1982.
21. This work was supported by PHS grant EY00014 and by NSF grant BNS 78-86171.

26 April 1982; revised 28 July 1982

## Sex Preselection in Mammals? Separation of Sperm Bearing Y and "O" Chromosomes in the Vole *Microtus oregoni*

**Abstract.** *The two sex determining sperm populations of the vole Microtus oregoni were separated according to DNA content by use of flow sorting instrumentation. Although the sperm were not viable, they should be useful for addressing the question of haploid expression of genes linked to sex chromosomes and for efficiently searching for biochemical markers that differentiate the two populations.*

The ability to influence the sex ratio of humans and agriculturally important animals would have profound social and economic impacts. Development of semen-based sex selection techniques has been impeded by the difficulty in identifying differences that might serve as a basis for enrichment or preferential inactivation of the sex-determining sperm populations. Although several physical, functional, and biochemical methods have been proposed and some patented (1), none has yet proven its efficacy in

large-scale trials. The only established difference on which to base sperm separation is chromosomal constitution. In most mammals, sperm containing the X chromosome lead to female offspring, and those with the Y to males. Typically the X and Y chromosomes differ in DNA content, resulting in a 3 to 4 percent difference between the X and Y sperm in humans and agriculturally important animals (2). Flow cytometric techniques that are sufficiently precise to resolve these populations in many species have

been developed (3, 4). We have used these techniques to determine the relative proportion of X and Y sperm in semen processed with several purported enrichment methods (5). None of the samples measured so far has been enriched.

It is reasonable to expect that appropriately adapted flow-sorting instrumentation could be used to separate sperm according to DNA content, and that these sperm might then be used to search for phenotypic differences that could be utilized for bulk separation of viable cells. However, current staining techniques adequate to resolve a 3 to 4 percent difference require decondensation of the highly compact sperm nucleus with proteolytic enzymes, substantially altering many biochemical components and generally disrupting sperm structure. The larger the difference in DNA content between the sex-determining sperm populations, the more biochemically conservative a staining protocol can be and still resolve them. For the vole *Microtus oregoni*, this difference is about 9 percent, more than double that of most mammals (6). We now report the successful sorting of sperm from *M. oregoni* using three preparative techniques with differing levels of cellular disruption. This represents a directly verified enrichment of the sex-determining sperm populations of a mammal.

*Microtus oregoni* is unusual in that it is a gonosomal mosaic (7); the gonadal and somatic cells have different chromosomal constitutions. Male somatic cells are XY, but the spermatogonia are OY. Thus, one of the sperm populations contains the Y chromosome and the other, here called "O," contains no sex chromosome. Only Y-linked genes are candidates for coding for markers that differentiate the two sperm classes in this animal. This may not be very different from what occurs in other mammals, since there is evidence that the X chromosome is normally inactivated during spermatogenesis (8).

In flow cytometry, a liquid suspension of single cells stained with a fluorochrome is made to flow in a thin stream that intersects a beam of excitation light. As each cell passes through the beam, optical detectors focused on the intersection convert the fluorescent flashes into electrical signals, which are analyzed with a multichannel analyzer. The data are displayed as histograms of the number of cells versus the brightness per cell. Multiple measurements on each cell result in multidimensional histograms.

Flow measurements of DNA content in mammalian sperm are particularly dif-